Minimization of defects generation in laser welding process of steel alloy for automotive application

Available online at www.sciencedirect.com

ScienceDirect

Procedia CIRP 115 (2022) 48–53

www.elsevier.com/locate/procedia

10th CIRP Global Web Conference – Material Aspects of Manufacturing Processes

Minimization of defects generation in laser welding process of steel alloy for automotive application

Giacomo Maculotti[a], Gianfranco Genta[a,*], Elisa Verna[a], Stefano Bonù[b], Luca Bonù[c], Roberto Cagliero[d], Maurizio Galetto[a]

[a]*Department of Management and Production Engineering, Politecnico di Torino, C.so Duca degli Abruzzi 24, 10129 Turin, Italy*
[b]*AGLA Power Transmission, Via Avigliana 9, 10051 Avigliana, Italy*
[c]*FORZA SMART INDUSTRY, Via XXV Aprile 11, 10051 Avigliana, Italy*
[d]*LBN Ricerca, Via Avigliana 2, 10057 Sant'Ambrogio di Torino, Italy*

* Corresponding author. Tel.: +39-011-090-7257. *E-mail address:* gianfranco.genta@polito.it

Abstract

Laser welding (LW) thanks to its flexibility, limited energy consumption and simple realization has a prominent role in several industrial sectors. LW process requires careful parameters' tuning to avoid generating internal defects in the microstructure or a poor weld depth, which reduce the joining mechanical strength and result in waste. This work exploits a supervised machine learning algorithm to optimize the process parameters to minimize the generated defects, while catering for design specifications and tolerances to predict defect generation probability. The work outputs a predictive quality control model to reduce non-destructive controls in the LW of aluminum for automotive applications.

Keywords: Laser welding; Defect; Microstructure.

1. Introduction

Among the various welding techniques available, laser welding (LW) is particularly attractive and performing compared to other joining technologies due to multiple factors. First of all, the simple setup does not require mechanical contact with the components to be welded, and ensures good final quality in terms of penetration depth, mechanical properties and stability, and also a higher welding speed [1]. Thus, due to its flexibility, effectiveness, and productivity, LW is a technology adopted for industrial applications in a variety of industries, e.g., aerospace, automotive, military, marine, and electronics [2].

Despite these benefits, the inherent chaotic nature of the laser system can generate several defects and non-conformities, e.g. sputter and weld break-ins, non-conforming laser weld depth and microstructural defects (porosity and/or cracks), thus requiring accurate quality control procedures. Post-process inspections are essential to inspect weld geometry and detect visible and internal defects, which are the major defects that companies would like to minimize to avoid scraps, reworks, and related poor-quality costs. Technologies used are eddy current, X-CT, ultrasonic techniques and, for innovative materials being developed or being introduced into a production line, destructive inspections requiring cross-sectioning and optical microscopes inspections. In particular, the penetration depth of the weld bead is one of the most critical parameters to ensure the final quality of the process and guarantee adequate mechanical properties [2]. Accordingly, identifying suitable post-inspection prediction models from

10.1016/j.procir.2022.10.048

process parameters to minimize generated defects is essential in pre-production and R&D. In the literature, several Machine Learning (ML) approaches are used to develop the model and to optimize the process parameters for improved LW process. These range from supervised to unsupervised techniques [2–4]. Typical approaches include Design of Experiments (DoE) and relevant analysis methodology, e.g. Response Surface Methodology (RSM) and Generalized Linear Model (GLM) [5], Gaussian Process Regression (GPR) [6], Kernel-based regression models [2,4], Support Vector Machine Regression (SVM or SVR) [7], and Classification and Regression Trees (CART) [8]. In addition, besides explainable artificial intelligence [9], also Genetic Programming (GP) and Neural Networks (NN) are adopted for welding applications [10].

In this paper, defects related to non-conforming weld depth and microstructural defects – with respect to specifications – are combined to derive an overall probabilistic estimate of occurrence of a (generic) defect in laser welded parts. In detail, a GLM and a CART will be used to model the relationship between process parameters and, respectively, weld depth and the presence of relevant microstructural defects. Then, a process optimization is performed to maximise the weld depth, considering the absence of microstructural defects. In such an optimized condition, a probability of occurrence of a non-conforming weld depth is derived. Both probabilities of weld depth and microstructural defects are combined to assess the overall quality of welded parts. The proposed approach is applied to a real industrial production of laser-welded steel parts for automotive applications.

The rest of the paper is structured as follows: Section 2 presents the considered case study, the experimental methodology, and the applied ML techniques to model and optimize the process and predict the probability of defects generation, while Section 3 presents and discusses the results, and Section 4 finally draws the conclusions.

2. Materials and Method

This study addresses the optimization of an industrially relevant case study, offered by AGLA Power Transmission, FORZA SMART INDUSTRY and LBN Ricerca, interacting companies in automotive field. The LW process is a manufacturing step for the support of a clutch disc in a CVT gearbox. LW is performed with state-of-the-art manufacturing equipment, i.e. a Ytterbium laser source, with tunable power up to 10 kW and a single-mode beam.

According to the literature, the customer requires the manufacturing of the component within tight specification of the minimum achievable laser weld depth S_n, and with strict control of the admissible type and the number of internal defects. The latter, in particular, can be of several types. In the considered case study, specifications were provided in terms of internal porosity and cracks. The former being acceptable up to a certain maximum threshold, and the latter never being tolerated. The weld geometry is an edge butt joint, cross section for the investigations have been carried out at 180° from the start of the welding process. For confidentiality reasons, the exact geometry of the manufactured component and the specified maximum tolerable porosity threshold are not disclosed.

2.1. Experimental set-up

A set of components was manufactured in different processing conditions to investigate the main process parameters, identified according to literature and company historical data. In particular, the laser power, the welding speed v and the focus offset F_O were considered, in accordance with industrial experience and literature [11,12]. Preliminary investigation considered also the effect of shielding gas flow, but a lack of significance resulted. A total of 88 parts were manufactured according to an unbalanced experimental design [13], due to company resource availability, with considered process parameters ranging over the levels reported in Table 1, and including some replication in randomly selected conditions. For confidentiality, the laser power is reported normalized to the laser spot area, i.e. as power density P_d.

Table 1 Considered parameters values in the implemented experimental design. Values of welding speed are in angular units as the welded component is axially symmetric. Power values are normalized to the laser spot area to avoid the disclosure of sensitive information and the power density is thus reported.

v / rad/s	P_d / W/mm²	F_O / mm
1.5	12025	-20
1.8	13086	-16
2.1	14147	-12
2.4	15031	-8
2.7	15915	-4
	16623	0
	17684	

Once the components were manufactured, they were cross-sectioned and prepared for inspection at optical microscopy by polishing with grit paper (240, 320, 800 and 1200) and diamond solution (6 µm, 3 µm and 1 µm). A Laborlux 12 ME Leitz with 50× magnification objective was used to measure the weld depth and investigate the presence of microstructural defects. Weld depth S_n is reported in millimetres, the presence of the two types of defects, i.e. internal porosity and cracks, were independently marked and then combined and reported as a dichotomous variable, defined as follows: X=1 for the presence of a microstructural defect and X=0 for the absence.

2.2. Statistical modelling

The collected data are analyzed and used to train a prediction model of the considered quality variables. In particular, the multivariable multivariate model in Eq. (1) is developed:

$$\begin{cases} S_n = g(P_d, v, F_O) \\ X = C(P_d, v, F_O) \end{cases} \quad (1).$$

Both the models are obtained by machine learning. As far as the function g is concerned, i.e. the prediction of the weld depth S_n, it is obtained by applying a generalized linear model (GLM) with variable reduction by stepwise method, considering an alpha-to-enter and an alpha-to-remove equal to

0.15 [14]. This allows defining a model capable of thoroughly and robustly describing the relationship between statistically significant process parameters, their interactions, and the weld depth, while avoiding overfitting. A GLM is adopted for its generality and its implementation simplicity [14–16]. The considered base model is polynomial of 3rd order with all interactions and parameters estimated by least square regression [15]. Similarly, by means of CART ensemble $\mathcal{C}$, prediction of relevant microstructural defects is obtained on the basis of process parameters is achieved. In particular, amongst the several statistical models for dichotomous variable, e.g. logistic regression, SVM and CART, the proposed approach allows suitable robustness, and flexibility while combining ease of readability and avoidance of overfitting by combining an ensemble of weak learners. The ensemble of trees is defined by a set of hyper-parameters, namely, the width and depth of each weak learner, the number of trees in the ensemble and the method of creation of the weak learners, e.g. boosting and bagging. The optimization of the hyperparameters set is a time and resource-intensive activity. In this study, a Bayesian optimization is adopted to explore the parameters' hyperspace to maximize the accuracy, i.e. minimize the RMSE [17,18].

2.3. Process optimization

Once the prediction model of Eq. (1) has been obtained, the welding process is optimized. This entails identifying the set of process parameters $\boldsymbol{\vartheta}_P^* = \{P_d, v, F_O\}^*$ that maximizes the weld depth in absence of microstructural defects, in other words:

$$\begin{cases} \boldsymbol{\vartheta}_P^* = \underset{\vartheta_P}{\operatorname{argmax}}(S_n = g(\boldsymbol{\vartheta}_P)) \\ 0 = \mathcal{C}(\boldsymbol{\vartheta}_P^*) \end{cases} \quad (2).$$

The problem is solved by a brute-force numerical evaluation of the process parameter space, i.e. evaluating Eq. (1) in all possible combinations of the process parameter space and then solving for Eq. (2) on the predicted responses. The possible combinations are limited to the set-up resolution of the industrial equipment.

2.4. Defect generation modelling

Although the process has been optimized, the model suffers from prediction uncertainty. This is liable for generating defects in the optimized process, resulting in scraps, rework and unnecessary costs [19]. Therefore, the probability of defects generation in optimized process conditions is essential to be estimated. In this work, two possible defects are considered: insufficient weld depth and presence of internal microstructural defects.

As far as the weld depth is concerned, the process optimization achieves the estimation of $S_n^* = g(\boldsymbol{\vartheta}_P^*)$. According to the GLM theory, this is a random variable normally distributed according to $N(S_n^*, u_{S_n^*}^2)$, having a probability density function $f(x; \mu = S_n^*, \sigma = u_{S_n^*})$. The variance of the distribution is obtained by combining the influence factors of the prediction model by the application of the law of uncertainty propagation as per the Guide to the expression of Uncertainty in Measurement (GUM) [20]:

$$u_{S_n^*}^2 = \sum_{i=1}^{k+3}\sum_{j=1}^{k+3} \frac{\partial g}{\partial x_i}\frac{\partial g}{\partial x_j} u(x_i, x_j) + MSE_g \quad (3.1)$$

$$x = \{\boldsymbol{a}, \boldsymbol{\vartheta}_P\} \quad (3.2)$$

$$MSE_g = \frac{\sum_{w=1}^{n}(\widehat{S_{n,w}} - S_{n,w})^2}{n-1} \quad (3.3),$$

where the propagation includes covariances of the GLM model parameters $\boldsymbol{a}$, the process parameters $\boldsymbol{\vartheta}_P$, and the variance of the model residuals, i.e. the model's mean squared error, to achieve the estimation of the S_n prediction interval [14,20,21]. Thus, the uncertainty is propagated considering k+3+1 influence factors, where k is the number of Eq. (1) parameters, 3 represents the process parameters, and 1 represents the model random fitting error. The latter is assumed to be normally distributed as $N(0, MSE_g)$.

As discussed in the Introduction, a tight control on the penetration depth is critical [2] and process specification that requires a minimum acceptable weld depth $S_{n,min}$ are stated, where the limit is strictly application dependent. Accordingly, a defect in optimized process condition is identified if $S_n^* < S_{n,min}$. Thus, the probability of generating a weld depth-defect is:

$$p_{def,S_n} = \mathbb{P}\left[S_n^* < S_{n,min}\right] = \int_{-\infty}^{S_{n,min}} f(x; S_n^*, u_{S_n^*})\, dx \quad (4).$$

The prediction model for the internal defects yields prediction results. The model validation, performed by a conventional 5-fold cross-validation, allows estimating true and false response rates, as per the tree diagram in Fig. 1.

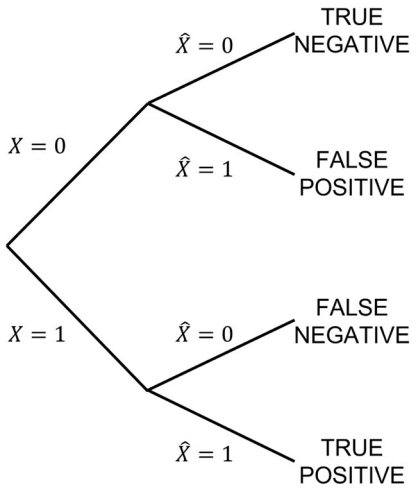

Fig. 1. Microstructural defect prediction response tree diagram, where $\hat{X}$ is the predicted response and X is the true response in the validation set.

The process optimization constraints the maximization of S_n to a predicted absence of defects, i.e. $\hat{X} = 0$. Under this assumption, the probability of defects generation in optimized process conditions is the false negative rate, i.e.:

$$p_{def,\mu structural} = \mathbb{P}\left[\hat{X} = 0 | X = 1\right] \quad (5).$$

Overall, the probability of generated defects in optimized process conditions is:

$$p_{def,tot} = p_{def,S_n} + p_{def,\mu structural} - p_{def,S_n} \cdot p_{def,\mu structural} \quad (6),$$

considering the defects to be independent. All computations are performed in *MATLAB* R2021b.

3. Results and discussion

3.1. Process and defects statistical modelling

The 88 components were manufactured and analyzed according to the methodology described in Section 2.1. Fig. 2 shows the results of the metallographic analysis identifying several types of defects, i.e. microporosity and cracks, as well as other components presenting no defects. The weld depth S_n was measured, and these results were exploited to train the prediction models as per the discussion in Section 2.2.

The main effects plot in Fig. 3 justifies the choice of a 3rd order polynomial as base model for the stepwise variable reduction.

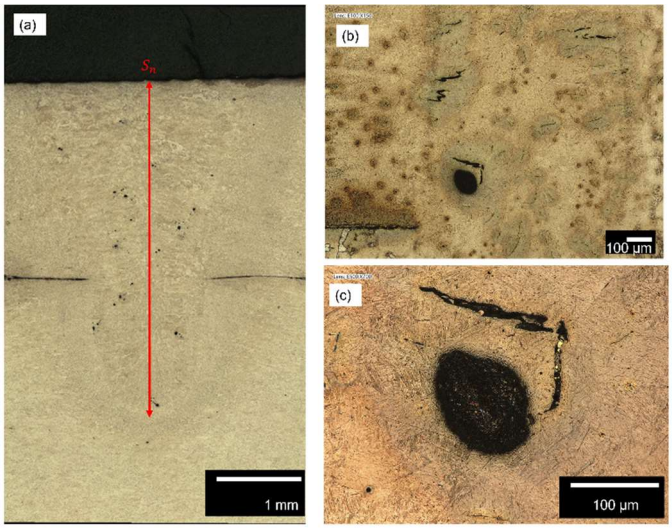

Fig. 2. Results of metallographic analysis at different magnification: (a) defective weld: porosities and cracks (image taken at 100× magnification) with indication of the measured weld depth S_n, (b-c) increasing magnification of the defects: cracks and porosity.

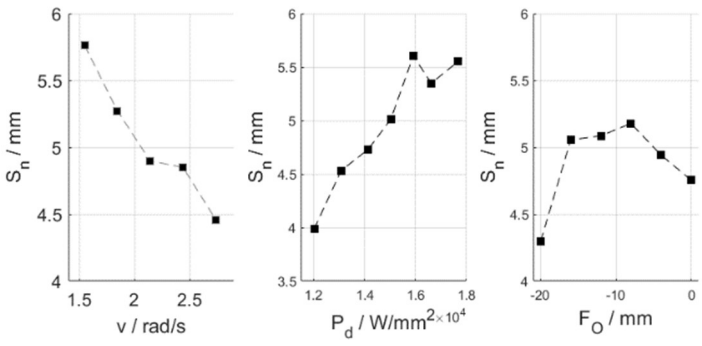

Fig. 3. Main effects plot for weld depth.

The GLM model for S_n is reported in Eq. (7), with parameters in homogeneous measurement unit to Table 1.

$$S_n = 0.1329 \cdot F_O + 8.4 \times 10^{-5} \cdot P_d + 10.129 \cdot v - 0.0091 \cdot F_O^2 + -1.9 \times 10^{-5} \cdot F_O \cdot P_d - 6.6654 \cdot v^2 + 1.246 \cdot v^3 \quad (7).$$

The model shows very good predictive and fitting capability, based on the predicted R-squared value of 92.5%. Additionally, the residuals were tested for normality, through a normal probability plot, shown in Fig. 4, and an Anderson-Darling test, which resulted in a p-value of 14.5% which cannot reject the null hypothesis of normality. Residuals showed a standard deviation of 0.2995 mm. Similarly, the prediction model for the internal defects was trained and validated. A CART based on an ensemble of week learners was selected and trained with hyperparameters optimization by Bayesian algorithm. The optimization selected a RUSBoosting for unbalanced classes [22], with 439 weak learners with a maximum number of nodes of 29. The model shows an adequate predictive capability, presenting an overall accuracy of 61.4%, and Table 2 reports the true and false positive and negative rates.

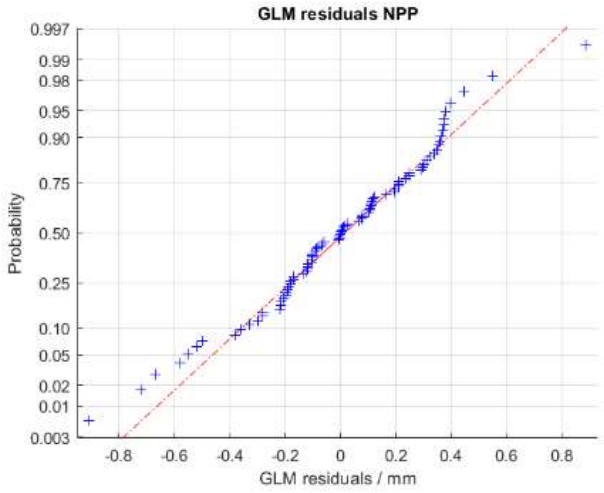

Fig. 4. NPP of GLM residuals for weld depth. Normality cannot be qualitatively disproved.

Table 2. True and false prediction rates of microstructural defects (see Fig. 1).

		$\hat{X}$	
		0	1
X	0	0.2954	0.2387
	1	0.1477	0.3182

3.2. Process optimization

The process was optimized exploiting the trained model defining Eq. (1) to solve for the best process parameters set $\boldsymbol{\vartheta}_P^*$ according to the methodology described in Section 2.3. The optimization is carried out seeking the parameters within the maximum process parameters window defined by the experimental plan. Fig. 5 shows the response surfaces for the model in Eq. (1), and the location of the optimized process parameters set $\boldsymbol{\vartheta}_P^*$, which is also reported in Table 3.

The obtained results in Eq. (7) can be explained on the basis of the weld physics. A suitable parameter to support such discussion is the Energy input, $E = {}^{P_d}/_{V}$, and the Energy density, i.e. $E_d = {}^{E}/_{A_{FO}}$, that is the Energy input normalized by the focal spot area [23]. Greater energy input ensures a larger penetration, which is consistent with the obtained results in Eq. (7) and Fig. 3. Accordingly, process optimization maximizes the power, while minimizing the speed and the focus offset is chosen so that the minimal weld spot area results.

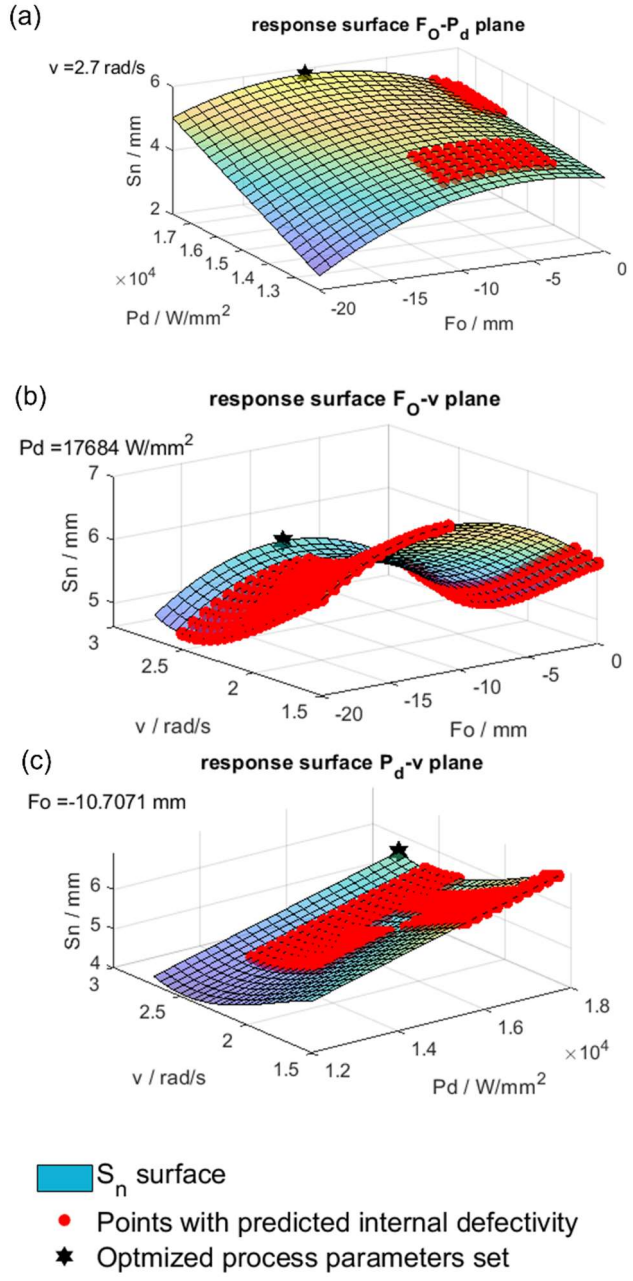

Fig. 5. Surface plots of the weld depth as a function of process parameters. In each of the represented surfaces, the third variable is set at the optimized value. Red dots are process parameters resulting in predicted internal defectivity. Black star is the optimized process parameter set.

Physics-based explanation of the obtained results in the case of internal defects is more challenging. In fact, it highlights on the shortcomings of the mathematical black-box approach here exploited, for it cannot relate physics of the process. The chosen physics modelling and the selected internal defects quality variable allow only partial insights on the physical relationship. In particular, the internal defects include cracks, that are never tolerated and often due to thermal gradient [24]. High gradient is generated by high power and low speed [25], as it is consistently shown in Fig. 5.

Indeed, the considered methodology presents shortcomings that currently being developed Physics-based Artificial Intelligence modelling will overcome [26,27]. However, the presented approach offers a simple black box modelling tool to optimize relevant process parameters to industrial practitioners, who might be not interested in deep understanding of the process physics.

Table 3. Results of process optimization (the predicted internal defect is not present, i.e. $\hat{X}^* = 0$).

P_d^* / W/mm²	F_O^* / mm	v^* / rad/s	S_n^* / mm
17684	-10.7071	2.7	5.813

3.3. Probability of defects generation

The optimized model was exploited to study the probability of defect generation.

Firstly, the generation of a non-conforming weld depth is analyzed. The uncertainty was propagated in the model of Eq. (7), considering the variance and covariance of the estimated parameters, including the contribution of the fitting error, modelled as white noise with MSE_g =0.0897 mm². Contribution from the model regressors, i.e. the process parameters, was modelled as a uniform distribution, with range of variability equal to twice the resolution allowed by the machine when setting up the process.

The uncertainty propagation results in a standard uncertainty $u_{S_n^*}$ = 0.305 mm. As a reference, the resulting expanded uncertainty prediction interval, evaluated with a coverage factor equal to 2, approximating a 95% confidence interval, is $S_n^* = (5.813 \pm 0.610)$ mm.

Consequently, as per Eq. (4), the probability of generating a defect related to the weld depth is $p_{def,S_n} = 1.30 \times 10^{-9}$, considering a $S_{n,min}$= 4 mm.

The probability of generating an internal defect, i.e. crack or porosity, is obtained, as per the discussion in Section 2.4, directly from Table 2, as $p_{def,\mu structural} = 0.1477$.

Therefore, in optimized process conditions, the probability of defect generation is $p_{def,tot} = 14.8\%$. Thus, since p_{def,S_n} is almost negligible, the overall probability of occurrence of a defect is mainly due to false negative prediction rates of microstructural defects.

4. Conclusions

Laser welding is a promising technique adopted in manifold sectors including aerospace, shipbuilding and automotive thanks to its flexibility, limited energy consumption and simple realization. Although the parameters used to manufacture laser-welded parts are optimized, the inherent uncertainty of the process can lead to defects and non-conformities. In particular, non-conforming laser weld depth and microstructural defects (porosity and/or cracks) are the major defects that companies

would like to minimize to avoid scraps, reworks, and related poor-quality costs.

The aim of this paper is to quantify the probability of occurrence of defects in laser-welded parts when process and related parameters are optimized. Both defects related to non-conforming weld depth and microstructural defects are considered. For modeling the relation between weld depth and microstructural defects with process parameters, a General Linear Model with variable reduction by stepwise method and a Classification and Regression Trees are adopted, respectively. Then, the weld depth is maximized in absence of microstructural defects to derive the set of optimal parameters. According to specifications, in such an optimized condition, the probability of non-conforming weld depth is estimated, and combined with false negative predictions of microstructural defects. The resulting overall probability defines the probability of occurrence of a (generic) defect in laser-welded parts. The description is supported by a real case study in the automotive field. According to the experimental results, the main findings can be summarized as follows:

- The probability of generating a defect related to the weld depth may be considered negligible.
- The probability of generating an internal defect, i.e. crack or porosity, is approximately 15%.
- In optimized process conditions, the probability of defect generation is mainly due to false negative prediction rates of microstructural defects and thus reaches about 15%.
- The combination of probabilities of non-conforming weld depth and false negative predictions of microstructural defects represents an innovative aspect of this study that enables a holistic prediction of the quality of laser-welded parts.

The prediction models developed in this study and the probabilities estimated enable engineers to predict defects occurring in laser-welded parts and accordingly plan and design effective quality controls to achieve the goals of zero-defect manufacturing.

Acknowledgements

The authors would like to thank Miss G. Di Paola and Mr. L. Bonamassa for their support in the experiments and preliminary data analysis.

References

[1] Jäger M, Humbert S, Hamprecht F. A Sputter tracking for the automatic monitoring of industrial laser-welding processes. IEEE Trans Ind Electron 2008;55:2177–84.
[2] Stavridis J, Papacharalampopoulos A, Stavropoulos P. Quality assessment in laser welding: a critical review. Int J Adv Manuf Technol 2018;94:1825–47.
[3] Rishikesh Mahadevan R, Jagan A, Pavithran L, Shrivastava A, Selvaraj SK. Intelligent welding by using machine learning techniques. Mater Today Proc 2021;46:7402–10.
[4] Cai W, Wang J, Zhou Q, Yang Y, Jiang P. Equipment and machine learning in welding monitoring: A short review. ICMRE 19 Proc. 5th Int. Conf. Mechatronics Robot. Eng., 2019, p. 9–15.
[5] Gagliardi F, Navidirad M, Ambrogio G, Misiolek WZ. Effect of material properties and process parameters on quality of friction stir forming. J Manuf Process. 2021;70:553–9.
[6] Wu J, Zhang S, Sun J, Zhang C. Data-driven multi-objective optimization of laser welding parameters of 6061-T6 aluminum alloy. J Phys Conf Ser. 2021;1885.
[7] Zhang F, Zhou T. Process parameter optimization for laser-magnetic welding based on a sample-sorted support vector regression. J Intell Manuf. 2019;30:2217–30.
[8] Zhang Z, Huang Y, Qin R, Ren W, Wen G. XGBoost-based on-line prediction of seam tensile strength for Al-Li alloy in laser welding: Experiment study and modelling. J Manuf Process. 2021;64:30–44.
[9] Rudin C. Stop explaining black box machine learning models for high stakes decisions and use interpretable models instead. Nat Mach Intell. 2019;1:206–15.
[10] Kim KY, Ahmed F. Semantic weldability prediction with RSW quality dataset and knowledge construction. Adv Eng Informatics. 2018;38:41–53.
[11] Sathish T, Sevvel P, Sudharsan P, Vijayan V. Investigation and optimization of laser welding process parameters for AA7068 aluminium alloy butt joint. Mater Today Proc. 2020;37:1672–7.
[12] Abioye TE, Mustar N, Zuhailawati H, Suhaina I. Parametric analysis of high power disk laser welding of 5052-H32 aluminium alloy. Mater Today Proc. 2019;17:599–608.
[13] Montgomery DC. Design and Analysis of Experiments New York; John Wiley & Sons; 1991.
[14] Galetto M, Genta G, Maculotti G, Verna E. Defect Probability Estimation for Hardness-Optimised Parts by Selective Laser Melting. Int J Precis Eng Manuf. 2020;21:1739–53.
[15] Montgomery D, Runger G, Hubele N. Engineering statistics. New York: John Wiley & Sons Inc.; 2010.
[16] Murphy KP. Machine Learning: A Probabilistic Perspective. Cambridge, MA: The MIT Press; 2012.
[17] Gelbart MA, Snoek J, Adams RP. Bayesian optimization with unknown constraints Uncertain. Artif Intell - Proc 30th Conf UAI 2014 2014:250–9.
[18] Gu P, Zhu C, Mura A, Maculotti G, Goti E. Grinding performance and theoretical analysis for a high volume fraction SiCp/Al composite. J Manuf Process. 2022;76:796–811.
[19] Galetto M, Verna E, Genta G, Franceschini F. Uncertainty evaluation in the prediction of defects and costs for quality inspection planning in low-volume productions. Int J Adv Manuf Technol. 2020;108:3793–805.
[20] JCGM 100:2008 Evaluation of Measurement Data — Guide to the Expression of Uncertainty in Measurement (GUM). Sèvres, France: JCGM.
[21] Barbato G, Genta G, Cagliero R, Galetto M, Klopfstein MJ, Lucca DA, Levi R. Uncertainty evaluation of indentation modulus in the nano-range: Contact stiffness contribution. CIRP Ann - Manuf Technol. 2017; 66:495–8.
[22] Seiffert C, Khoshgoftaar TM, Van Hulse J, Napolitano A. RUSBoost: Improving classification performance when training data is skewed. Proc - Int Conf Pattern Recognit, 2008:8–11.
[23] Abioye TE, Farayibi PK, Clare ATA. comparative study of Inconel 625 laser cladding by wire and powder feedstock. Mater Manuf Process. 2017;32:1653–9.
[24] Costa A, Miranda RM, Quintino L. Materials behavior in laser welding of hardmetals to steel. Mater Manuf Process. 2006;21:459–65.
[25] Nunes AC. An Extended Rosenthal Weld Model: A moving heat source weld model can be extended to include effects of phase changes and circulations in the weld pool. Am Weld Soc. 1983;6:165–170.
[26] Karniadakis GE, Kevrekidis IG, Lu L, Perdikaris P, Wang S, Yang L. Physics-informed machine learning. Nat Rev Phys. 2021;3:422–40.
[27] Gunasegaram DR, Murphy AB, Barnard A, DebRoy T, Matthews MJ, Ladani L, Gu, D. Towards developing multiscale-multiphysics models and their surrogates for digital twins of metal additive manufacturing. Addit Manuf. 2021;46:102089.